CHEMICAL WEATHERING OF CRYSTALLINE ROCKS IN THE CATCHMENT AREA OF ACIDIC TICINO LAKES, SWITZERLAND

Rudolf Giovanoli,[1] Jerald L. Schnoor,[2] Laura Sigg,[3]
Werner Stumm,[3] and Jürg Zobrist[3]

[1] Laboratory of Electron Microscopy, Institute of Inorganic Chemistry
University Bern, CH-3000 Berne 9, Switzerland

[2] Department of Civil and Environmental Engineering, University of Iowa
Iowa City, Iowa 52242

[3] Swiss Federal Institute for Water Resources and Water Pollution Control
EAWAG, Swiss Federal Institute of Technology, ETH
CH-8600 Duebendorf, Switzerland

Abstract—Atmospheric acidic deposition introduces hydrogen ions to terrestrial and aquatic ecosystems, which become partially neutralized by chemical weathering. In the southern Alps of Switzerland, small catchments containing little or no soil and lacking carbonate minerals represent sensitive hydrological settings in which the relationship between alteration of granitic gneiss by acid deposition and the resulting composition of lake waters can be studied. Transmission and scanning electron microscopy, coupled with X-ray powder diffraction of lake sediments from such areas showed mainly unaltered minerals from parent rocks and no secondary silicate minerals. Element mapping indicated noncrystalline aluminum hydroxide as a product of the chemical weathering of silicates. Noncrystalline iron hydroxide was also observed. Mass balance calculations and the stoichiometry of suitable chemical reactions representing the weathering processes were used to derive a plausible reaction sequence on the interaction of the predominant reactive rock minerals with acid precipitation that accounted for the measured chemical composition of the acid lakes.

Key Words—Acid precipitation, Aluminum hydroxide, Gneiss, Iron hydroxide, Weathering.

INTRODUCTION

Chemical weathering is an important feature of the global hydrogeochemical cycle of elements. During chemical weathering, rocks and primary minerals become transformed to solutes and soils and, eventually, to sediments and sedimentary rocks. In this cycle, water occupies a central position, serving both as a reactant and as a transporting agent of suspended and dissolved material. The sea is the ultimate receptacle of weathered material, and the atmosphere provides a reservoir of weak acids (CO_2) and oxidants.

Acid atmospheric deposition results from the anthropogenic disturbance of cycles that couple atmosphere, land, and water. Redox conditions in the atmosphere are modified by the oxidation of carbon, sulfur, and nitrogen which result from fossil fuel combustion. Oxidation reactions exceed reduction reactions in the elemental cycles, and, coupled with the change in the electron balance, a net production of hydrogen ions in atmospheric precipitation is a necessary consequence (Stumm *et al.*, 1983, 1987a). The disturbance is transferred to the terrestrial and aquatic environment where, eventually, acidity is neutralized by bases supplied by the weathering of rocks or by ion exchange, and by reduction reactions that consume protons (Schnoor and Stumm, 1985, 1986). Depending on their hydrologic and geologic characteristics, chemical weathering in some catchments is unable to supply sufficient degradation products from rock-forming minerals to neutralize incipient acid deposition and protons supplied by other chemical processes. In such areas, the stream or lake within the catchment becomes acidified.

In this investigation, the relationship between rock weathering and resulting water chemistry in an area of the southern Alps in Ticino, Switzerland, was studied. On the basis of quantitative analyses of rocks and precipitation and water chemistry, plausible weathering reactions based on stoichiometry were established. Transmission and scanning electron microscopy, energy-dispersive X-ray spectrometry, and electronic processing of X-ray element distribution maps were used to identify reactant minerals and weathering products. In previous research, we reported the chemical composition of lake waters and their sensitivity to acidification (Schnoor and Stumm, 1985, 1986; Zobrist *et al.*, 1987), the aqueous phase chemistry of fog and wet deposition (Stumm *et al.*, 1983; Sigg *et al.*, 1987), and the principles of chemical weathering (Furrer and Stumm, 1986; Stumm *et al.*, 1987b). Here, we focus on weathering in the field and demonstrate which minerals are important in neutralization and secondary mineral-formation processes.
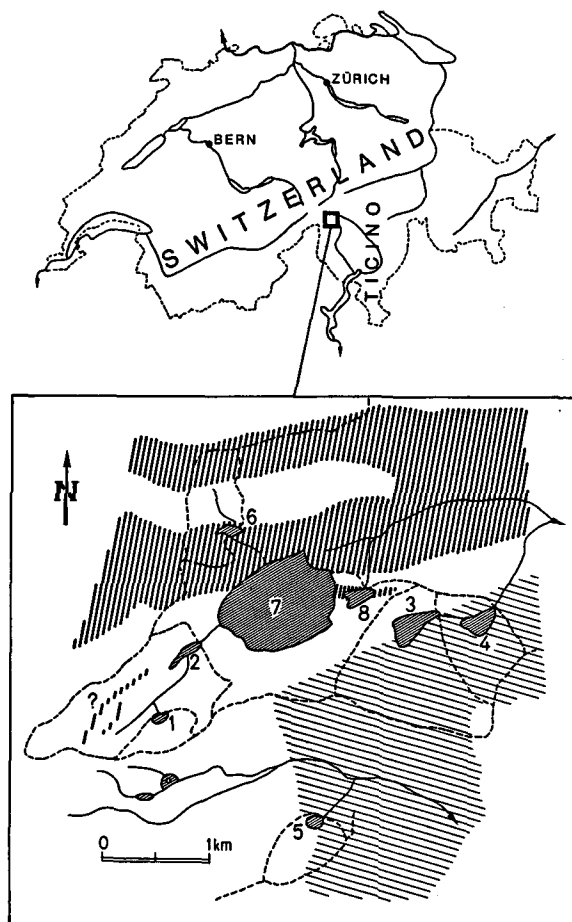
521

Figure 1. Map of the area studied in the Canton of Ticino, Switzerland. Lakes = 1, Cristallina; 2, Piccolo Naret; 3, Superiore; 4, Inferiore; 5, Zota; 6, Val Sabbia; 7, Naret (dammed lake with additional inflow); 8, Scurio. ----- = boundary of drainage area. Bedrock: □ gneiss, mainly alkali feldspar and plagioclase; ▨ granitic gneiss, mainly alkali feldspar and oligoclase; ▥ calcareous mica schist (Bündnerschiefer), including dolomite and calcitic sandstone.

MATERIALS AND METHODS

Site description

The site is in the Alps of southern Switzerland in the Canton of Ticino, at the top of the Maggia Valley (N46°28′, E8°33′; see Figure 1). The bedrock in the main part of the area consists of crystalline rock of pre-Carboniferous age, with granite and metamorphic gneiss predominating (Maggia tectonic unit). Some parts of the catchment areas are underlain by "Bündnerschiefer", schistose rocks of Jurassic-Cretaceous age, and a Jurassic unit containing dolomite and some calcite-bearing sandstone. The study area is at 2070–2550 m elevation and is characterized by sparse vegetation (no trees), thin soils, and steep slopes. Bedrock is exposed in more than 50% of the catchment area.

The catchment receives an average of 2.0–2.4 m of precipitation each year, of which more than half falls as snow. The average pH of the precipitation ranges from 4.5 to 5.5. The most acidic lakes, Lake Cristallina and Lake Zota (pH < 5.3), are in the catchment area that consists predominantly or exclusively of crystalline rock.

Chemical composition and mineral analysis

Elemental analyses of the rock and sediment samples (Table 1) were obtained by X-ray fluorescence using a routine procedure for rock analysis. All samples were examined by X-ray powder diffraction (XRD) in a high-resolution Guinier-NONIUS camera (Mark IV) with $CuK\alpha_1$ and $FeK\alpha_1$ radiation, using a focussing monochromator.

Electron microscopy and X-ray spectrometry

Sample 3 (Table 1) was investigated in great detail. It is a gneiss, weathered on the outside but fairly intact in its center. The rock was broken in half, and a sample from the center and from the weathering rind were glued directly on an aluminum sample holder and sputtered with gold. The morphology of these two specimens was investigated in a JEOL JSM 840 scanning electron microscope (SEM). Smaller samples were glued on a graphitized aluminum foil of 3-mm diameter and analyzed in a HITACHI H-600-2 transmission electron microscope in the scanning mode. EDX (energy dispersive X-ray) data were recorded using a TRACOR TN 5400 X-ray spectrometer.

The weathering products (sediment samples from Lake Cristallina and Lake Zota) were prepared in a suspension in distilled water and dispersed in an ultrasonic bath. The suspension was then directly transferred to carbon films on a bronze grid. Suitable transmission electron micrographs were taken and complemented with selected-area electron diffraction. These specimens were first examined using a BEAM-SCAN unit attached to the TRACOR TN 5400 spectrometer in the scanning transmission mode. The $K\alpha$ lines of Si, Ca, Al, K, and Fe excited by the electron beam were then recorded. This technique allowed the topographic location of these elements to be detected. Using a transmission-scanning mode picture as reference, these X-ray dot maps indicated unambiguously which elements were present in which crystal of the examined field. The X-ray maps were electronically processed to remove background radiation and other spurious effects.

Water analysis

Ion chromatography was used to analyze solutions for SO_4^{2-}, NO_3^-, and Cl^-; Ca^{2+}, Mg^{2+}, K^+, Na^+, and dissolved Al^{3+} were measured by atomic absorption. The samples for Al determination were filtered immediately after sampling and subsequently acidified. Because the lake waters had low ionic strength and

Table 1. Chemical analyses of rock and sediment samples.[1]

	Rock sample								Sediment sample	
Sample: Description: Location (lake):	1 Gneiss Cristal- lina	2 Weathered gneiss Piccolo Naret	3 Weathered gneiss Piccolo Naret	4 Dolomite Sabbia	5 Bündner- schiefer Sabbia	6 Gneiss Laghetto	7 Sandstone with calcite Scurio	8[2] Granitic gneiss Zota	9 Coarse Zota	1 Coarse Cristal- lina
Fe_2O_3	4.6	1.2	0.32	0.57	9.6	3.4	0.52	2.4	4.9	5.5
TiO_2	0.46	0.06	0.05	0.06	1.0	0.39	0.05	1.0	0.61	0.70
CaO	4.3	0.37	1.5	51.5	4.7	2.5	53.7	2.2	2.5	2.2
MnO	0.08	nd	nd	0.02	0.11	0.05	0.03	0.10	0.05	0.06
P_2O_5	0.10	0.15	0.21	0.07	0.19	0.11	0.07	0.07	0.17	0.19
K_2O	2.6	2.8	1.8	0.69	4.0	1.6	2.0	3.9	3.5	3.1
SiO_2	67.9	77.9	79.6	7.4	52.8	70.6	37.1	71.9	65.7	65.0
Al_2O_3	15.7	13.5	13.7	1.7	24.2	15.6	4.4	14.3	17.7	18.7
MgO	1.7	0.01	0.04	38.0	2.6	1.2	1.6	0.61	2.1	2.1
Na_2O	2.6	4.0	2.8	nd	0.79	4.6	0.57	3.2	2.8	2.5
Ignition loss (1150°C)	0.71	0.90	0.96	44.3	3.6	0.72	30.4	0.5	6.6	6.3

[1] Results from analysis by the Swiss Federal Laboratories for Materials Testing and Research (EMPA), given in g/100 g (%) of the ignited samples.
[2] From Günthert et al. (1976).

were poorly buffered, pH was measured in the field and in the laboratory after adjusting the ionic strength with KCl and calibrating the system at the temperature of the samples in the field. Acidity and alkalinity were determined in the laboratory by Gran titrations (Johnson and Sigg, 1985).

Stoichiometry of weathering reactions

Table 2 gives representative equations for the chemical dissolution of minerals; these equations were used to establish mass balances by which the impact of the weathering reactions on water chemistry was assessed. Chemical weathering of aluminum silicates is usually incongruent and occurs by a sequence of reaction steps. The literature proposes essentially two types of weathering reactions: (1) The dissolution of aluminum silicates is accompanied by the formation of secondary minerals, such as kaolinite. The occurrence of such reaction products are in agreement with thermodynamic considerations (Garrels and Christ, 1965) and certain field observations (e.g., Tardy, 1971; Keller, 1978). (2) The weathering process leads directly to aluminum (hydr)oxides and silicic acid. The dominant weathering process is a slight alteration of large volumes of rock without the formation of secondary silicate minerals (Miller and Drever, 1977). Different environmental conditions and hydraulic regimes may determine whether or not secondary silicate minerals are formed. In the present study, crystalline secondary minerals were not found as weathering products.
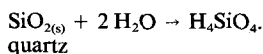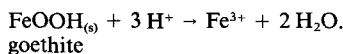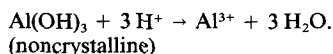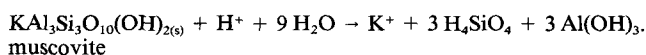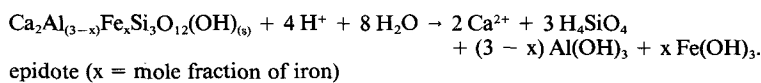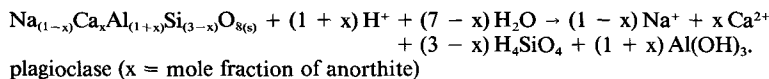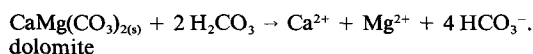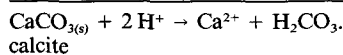
RESULTS AND DISCUSSION

Rock chemistry

The predominant bedrock in the vicinity of Lake Cristallina is represented by the gneisses of samples 1

and 6 in Table 1. These two rocks have similar elemental compositions, with the exception of the Ca:Na: K mole ratios, which are about 3:6:2 and 3:9:2, respectively. Sample 8 represents the granitic gneiss in the eastern part of the catchment area of Lake Zota. XRD analyses of samples 1 and 6 showed the presence of major amounts of quartz, plagioclase, feldspar, biotite, muscovite, and some chlorite. Günthert et al. (1976) described the mineral and element composition of the rocks in the adjacent crystalline area. The combination of their data with the present rock analysis gives the following mineral composition: plagioclase 35–45% (anorthite 20–30%), quartz 25–35%, K-feldspar 10–14%, biotite 8–14%, muscovite 3–5%, and epidote 2–4%. The granitic gneiss in the catchment area of Lake Zota has a somewhat larger K-feldspar and a smaller quartz content.

Other bedrock samples are listed in Table 1 for illustrative purposes. The light-colored weathered gneiss at Lake Piccolo Naret (samples 2 and 3) is deficient in Ca and Fe, but richer in silica than the gneisses of samples 1 and 6. Mineralogically, sample 3 consists of quartz, plagioclase, and muscovite. Because they represent only a relatively small outcrop area, the rocks represented by samples 2 and 3 probably contributed little to the water chemistry of the Lakes Cristallina or Piccolo Naret. Sample 4 illustrates the Jurassic dolomites. XRD showed that this rock is nearly pure dolomite with some quartz and traces of calcite and muscovite. It supplied Ca^{2+}, Mg^{2+}, and substantial alkalinity to Lake Sabbia via chemical weathering. Dolomites and calcite, however, were not found in the catchments of the Lakes Cristallina and Zota. Sample 5 is from Bündnerschiefer unit and contains quartz, muscovite, and chlorite, with traces of feldspar and calcite. Sample

Table 2. Dissolution reactions in approximate rank order for ease of weathering.[1]

$CaCO_{3(s)} + 2\,H^+ \rightarrow Ca^{2+} + H_2CO_3$.
calcite

$CaMg(CO_3)_{2(s)} + 2\,H_2CO_3 \rightarrow Ca^{2+} + Mg^{2+} + 4\,HCO_3^-$.
dolomite

$Na_{(1-x)}Ca_xAl_{(1+x)}Si_{(3-x)}O_{8(s)} + (1 + x)\,H^+ + (7 - x)\,H_2O \rightarrow (1 - x)\,Na^+ + x\,Ca^{2+}$
$+ (3 - x)\,H_4SiO_4 + (1 + x)\,Al(OH)_3$.
plagioclase (x = mole fraction of anorthite)

$Ca_2Al_{(3-x)}Fe_xSi_3O_{12}(OH)_{(s)} + 4\,H^+ + 8\,H_2O \rightarrow 2\,Ca^{2+} + 3\,H_4SiO_4$
$+ (3 - x)\,Al(OH)_3 + x\,Fe(OH)_3$.
epidote (x = mole fraction of iron)

$KMg_xFe_{(3-x)}AlSi_3O_{10}(OH)_{2(s)} + (1 + 2x)\,H^+ + (9 - 2x)\,H_2O \rightarrow K^+ + x\,Mg^{2+}$
$+ 3\,H_4SiO_4 + Al(OH)_3 + (3 - x)\,Fe(OH)_2$.
biotite (x = mole fraction of magnesium)

$KAlSi_3O_{8(s)} + H^+ + 7\,H_2O \rightarrow K^+ + 3\,H_4SiO_4 + Al(OH)_3$.
orthoclase (K-feldspar)

$KAl_3Si_3O_{10}(OH)_{2(s)} + H^+ + 9\,H_2O \rightarrow K^+ + 3\,H_4SiO_4 + 3\,Al(OH)_3$.
muscovite

$Al(OH)_3 + 3\,H^+ \rightarrow Al^{3+} + 3\,H_2O$.
(noncrystalline)

$FeOOH_{(s)} + 3\,H^+ \rightarrow Fe^{3+} + 2\,H_2O$.
goethite

$SiO_{2(s)} + 2\,H_2O \rightarrow H_4SiO_4$.
quartz

[1] From greatest to least; these reactions could also be written, instead of with H^+ ions as reactants, with water and dissolved CO_2. In either scheme, the net result of the reaction is the same—cations (Ca^{2+}, Mg^{2+}, Na^+, K^+) are released, and alkalinity is produced via OH^- or HCO_3^- production or H^+ consumption. In all reactions, the equivalents of cations released are exactly balanced by the equivalents of acid consumed which corresponds to the alkalinity produced.

7 from Lake Scurio is a quartz sandstone cemented by calcite.

Feldspars, quartz, and mica were identified by SEM in the weathered rind of the gneiss sample 3. The micas were identified on the basis of their leafy or platy habit (Figure 2). Quartz was also easily identified by its conchoidal fracture and smooth surfaces. In addition, the EDX spectra clearly indicated these minerals by their elemental composition.

The surfaces of some white, macroscopic plagioclase grains were covered with what appeared to be etch pits. According to Blum and Lasaga (1987), the presence of etch pits suggests that defects in the crystal structure are sites of strong preferential dissolution during geochemical processes. As shown in Figure 3, the etch pits were arranged along subgrain boundaries. Deformed feldspars similar to those found in the present study have been shown to contain dislocations (Heggie and Zheng, 1987). Uniform distributions of etch pits have been described previously (Berner and Holdren, 1977; Fung and Sanipelli, 1982; Robert *et al.*, 1986). Various sizes of etch pits were noted. Some grains exhibited only one population of pits, whereas others showed two sizes (Figure 4), suggesting that the grains underwent one and two episodes of weathering, respectively

(Figure 4b). In all likelihood, the gneiss reacted along the grain boundaries, and little of the absolute mass was chemically dissolved; however, this specially selective reaction was enough to cause the gneiss to disintegrate into grains of the minerals of which it was composed and which are found in the sediments.

Some feldspar and quartz surfaces are brown and covered by a coating, as seen in the scanning electron microscope (Figure 5). The EDX spectrum of such a quartz grain is shown in Figure 5b. Si is the main element; Fe is also abundant. Red, iron-containing patches were found on the surface of sediments in the more acidic lakes and appear to be a noncrystalline ferric hydroxide. Crystalline iron oxyhydroxides were not identified in any of the samples. Thus, iron that dissolved from the rock appears to have been washed into the sediment.

Chemistry of lake sediments

Nine samples (three from Lake Zota and six from Lake Cristallina) were analyzed. The data given in Table 1 for samples 9 and 10 are representative of the elemental composition of the sediments in these two lakes. The sediment compositions are surprisingly similar to those of the gneiss and the granitic gneiss (sam-
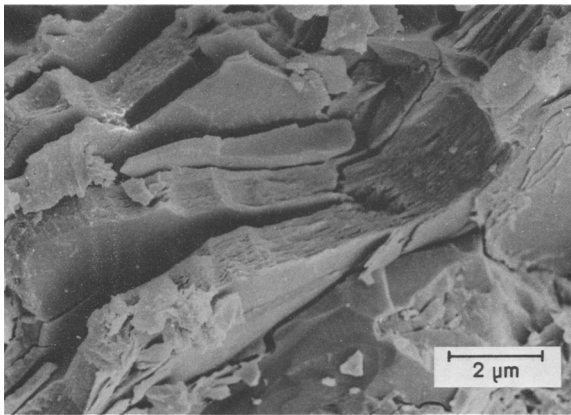
Figure 2.   Scanning electron micrograph of weathered gneiss, showing packs of mica splitting into sheets. Attack was apparently from edges and propagated through interlayer cleavage. Sheet surfaces appear clean and unattacked.

Figure 4.   Scanning electron micrographs of corroded feldspar grains, showing that shape of the etch pits depends on symmetry of attacked surface. (a), (c), and (d) show only one population of etch pits. (b) shows two populations (large and small), suggesting that this grain has been exposed to two periods of attack.

ples 1 and 8), although Al is enriched and Si is depleted in the sediments. The TEM/SEM and EDX data suggest different minerals in the different size fractions, but no difference was noted among the various samples as a function of depth (0–4, 4–8, 8–16 cm) in a core taken in Lake Cristallina.

The coarse size fraction contained quartz, feldspars, muscovite, and biotite (Figure 6), suggesting that this material was chiefly unaltered rock fragments from the catchment area. In the fine size fraction, slightly weathered biotite (Figure 7) and feldspars were detected. In addition, some illite and/or smectite and aggregations of noncrystalline ferric hydroxide and diatoms were found. No kaolinite was identified.

Although the elemental analysis indicates an enrichment in Al, no crystalline Al phase was observed in any of the samples. Neither XRD nor electron diffrac-

tion showed a separate Al hydroxide phase. The solubility measurements (Figure 11) give concentration values slightly greater than those expected for gibbsite, although this phase was not detected. Al dot maps of several samples were made using the BEAMSCAN attachment to the X-ray spectrometer. Some Al was noted in the remains of all muscovite and biotite grains, but typically Al was also distributed over the entire field of the sample grid. Figure 7 shows typical series of micrographs. An aggregation of particles is depicted in the scanning transmission mode and by means of Al (Figure 7b), Si (Figure 7c), and Fe (Figure 7d) dot maps. The (b) and (c) photos of each figure are not identical; however, they should be if Al and Si were constituents of the same mineral species. Thus, the Al is probably present as a noncrystalline phase, most probably a noncrystalline Al hydroxide. To check this conclusion, a solution having a total concentration of Al^{3+} of 10^{-4} M (pH 7) was investigated after drying on an electron microscope specimen grid. The electron microscope showed that the Al hydroxide was present
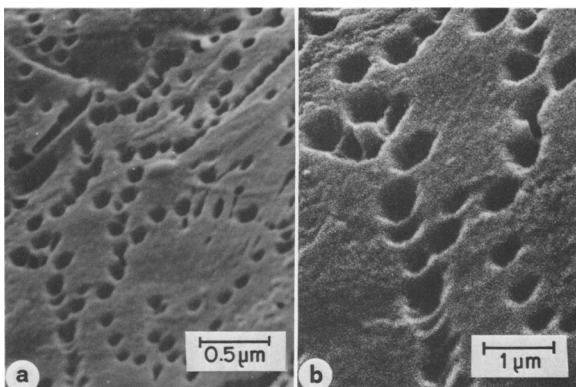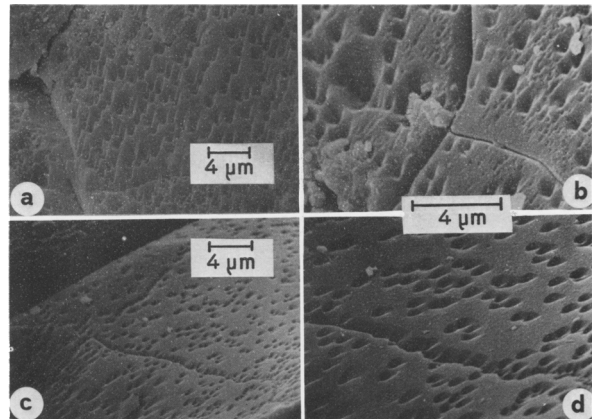

Figure 3.   Scanning electron micrograph of corroded feldspar grain. Same region in two enlargements showing the etch pits aligned along subgrain boundaries. Etch pits have narrow size distribution.
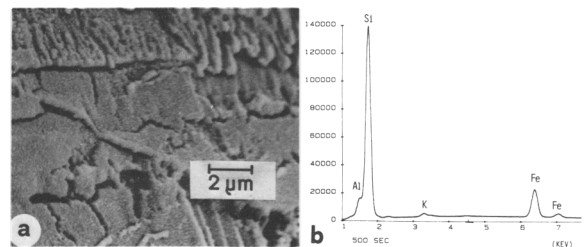

Figure 5.   Scanning electron micrograph of feldspar, entirely covered with brown, finely divided material (a), and energy-dispersive X-ray of a quartz grain nearby (also covered with the brown material), showing the FeKα and FeKβ lines (b).
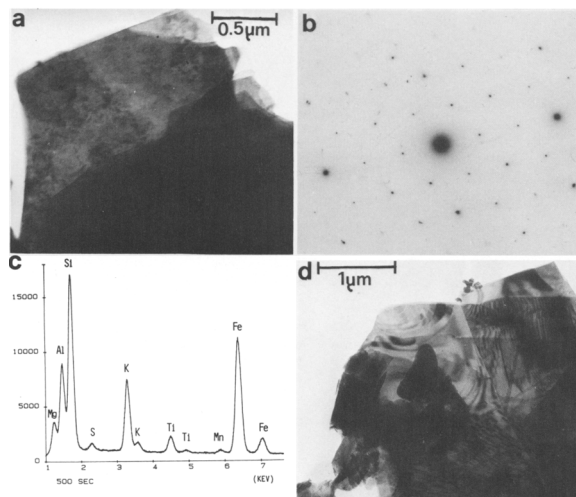
Figure 6. Lake sediment, coarse size fraction: (a) Transmission electron micrograph of biotite platelet (identified from element composition in the energy dispersive X-ray spectrum), and (b) its selected area electron diffraction pattern; (c) energy-dispersive X-ray spectrum of the same sample as in (a), with characteristic elements of biotite. (d) Transmission electron micrograph of muscovite platelet in the same sample; note typical Bragg fringes, indicating intact lattice. In (a) these Bragg fringes are intersected and indicate that the structure has undergone attack.

in this solution in colloidal form. Shadowing the grid with Cr at an incident angle of 45° made the colloid particles visible (Figure 8); they had a size of about 50–200 Å (Pavlova and Sigg, 1988).

Figure 8. Transmission electron micrograph of colloidal Al hydroxide particles, chromium shadowed at 45° incident angle; found after drying a drop of a solution of Al with total Al concentration 10^{-4} M and pH 7.

The ferric hydroxide was also amorphous to X-rays and aggregated to flakes. In the field, it is conspicuous by its orange color in patches on the surface of the lake sediment. The transformation of ferric hydroxide to goethite is strongly retarded by the presence of H_4SiO_4 (Cornell and Giovanoli, 1987).

The similarity in the chemical composition and mineralogy of the bedrock and the sediment was expected,
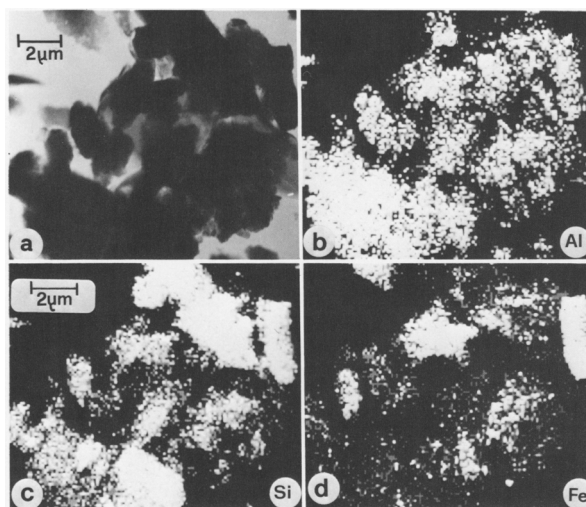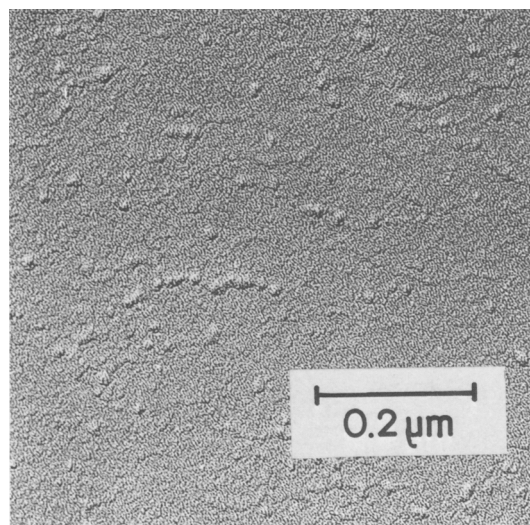

Figure 7. (a) Scanning transmission electron micrograph of decomposed biotite platelets in fine fraction of lake sediment. (b) Al dot map of same region, showing uniform distribution of Al. (c) Si dot map of same region, showing higher concentrations, mainly in grains in upper right corner and in lower middle part. (d) Fe dot map of same region, showing aggregations of formless iron hydroxide on right-hand side and in upper center of micrograph.
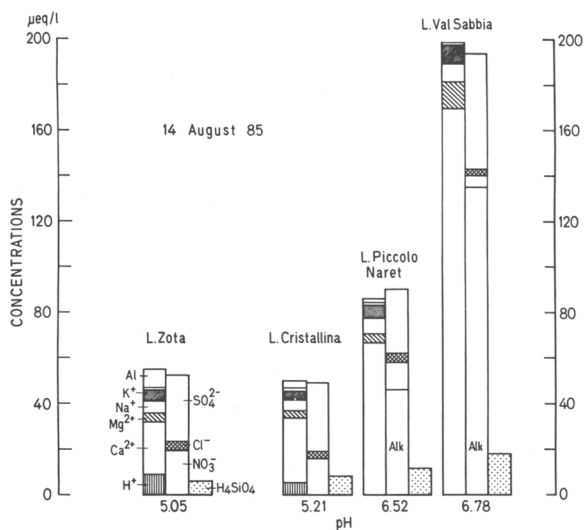

Figure 9. Comparison of water composition of four lakes influenced by different bedrocks in their catchments. Drainage areas of Lake Zota and Lake Cristallina contain only gneiss and granitic gneiss; that of Lake Piccolo Naret contains small amounts of calcareous schist; that of Lake Val Sabbia exhibits a higher proportion of schist.
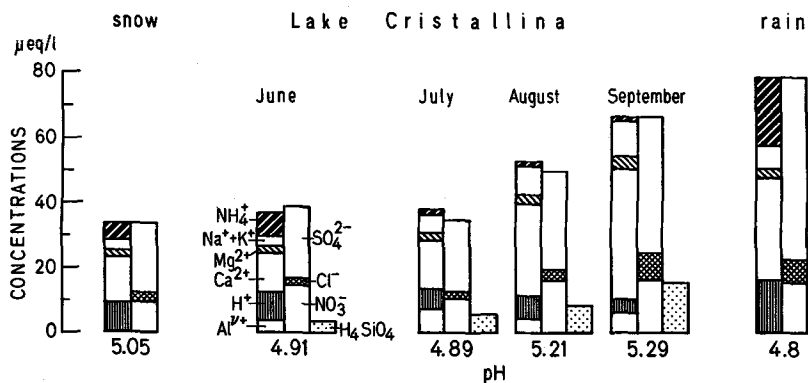
Figure 10. Evolution of water composition in Lake Cristallina during summer 1985. For comparison, compositions of snow and rain are shown.

inasmuch as mechanical weathering, most likely, facilitated by ice formation in the cracks of the rocks, contributed a large mass fraction of mostly unaltered minerals to the sediments.

Water chemistry

The composition of the water in these mountain lakes reflects the geology of their catchment areas. The composition of four different lakes, collected on the same sampling date (1985), are compared in Figure 9. The compositions of Lakes Cristallina and Zota, situated within a drainage area characterized by the preponderance of gneissic rocks and the absence of calcite and dolomite, and Lake Val Sabbia, the catchment area of which contains dolomite, are markedly different. The waters of Lake Cristallina and Lake Zota exhibit mineral acidity (i.e., caused by mineral acids and HNO_3), their calcium concentrations are 10–15 μmole/liter and their pH is <5.3. On the other hand, the water of Lake Val Sabbia is characterized by an alkalinity of ~130 μmole/liter and a calcium concentration of ~85 μmole/liter. The water of Lake Piccolo Naret is intermediate; its alkalinity is <50 μmole/liter and appears to have been influenced by the presence of some calcite or dolomite in its catchment area.

In Figure 10, the change in lake water composition for Lake Cristallina is shown for the period of one summer. Residual lake acidity was largest in late spring, when much of the acidity was eluted by the snow during warming and initial melting of its surface layers. In August, most of the snow in the drainage area had disappeared, and the effect of weathering was more important.

Weathering processes regulating the chemical water composition

On the basis of simple mass-balance considerations plausible reconstructions were attempted for the contribution of the various weathering processes responsible for the residual water composition of the acidic

Lakes Cristallina and Zota. Stoichiometric reactions are presented in Table 3 for the interaction of acidic deposition (snow melt) with weatherable minerals in the drainage area. The composition of atmospheric deposition results generally from the interactions of strong acids (H_2SO_4, HNO_3), bases (NH_3) and wind-blown dust and aerosols ($CaCO_3$, $MgCO_3$, NH_4NO_3, NaCl, KCl) (Stumm *et al.*, 1983). The values given in Table 3 for atmospheric deposition were compiled from data measured regularly at a sampling station 10 km west of Lake Cristallina (Mosello and Tartari, 1987); they
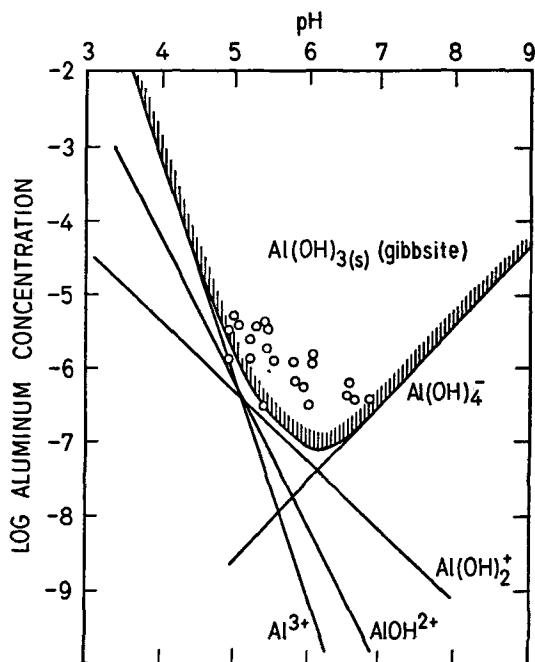

Figure 11. Solubility diagram of gibbsite showing pH-dependence of different Al species (lines). Al concentrations measured in these alpine lakes (○) agree reasonably well with theoretical equilibrium concentrations (calculated according to May *et al.*, 1979).

Table 3. Possible reaction sequences coupled with stoichiometric calculations for establishing chemical composition of Lake Cristallina and Lake Zota.

	Substances produced or consumed (−)											
Reactants	H$^+$	Na$^+$	K$^+$	Ca^{2+}	Mg^{2+}	NH$_4^+$	Al(OH)$_{3-\nu}^{\nu+}$	SO$_4^{2-}$	NO$_3^-$	Cl$^-$	H$_4$SiO$_4$	[Al(OH)$_3$]$_s$
Genesis of precipitation (wet and dry deposition)												
					(µeq/liter)						(µmole/liter)	
31 µeq H$_2$SO$_4$ ⎱ acids	31							31				
11 µeq HNO$_3$ ⎰	11								11			
3 µeq NaCl ⎱ "dust"		3								3		
2 µeq KCl ⎰			2							2		
19 µeq CaCO$_3$ ⎱	−19			19								
2 µeq MgCO$_3$ ⎬ bases	−2				2							
10 µeq NH$_3$ ⎰	−10					10						
Resulting composition	11	3	2	19	2	10	<1	31	11	5	<1	<1
After evaporation[1]	16	4	3	27	3	14	<1	44	16	7	<1	<1
Lake Cristallina Weathering reactions												
1 µmole calcite	−2			2								
4 µmole plagioclase (x = 0.25)	−5	3		2							13	5
2 µmole epidote (x = 0.5)	−8			8							6	5
1 µmole biotite (x = 0.5)	−2		1		1						3	1
1 µmole K-feldspar	−1		1								3	1
Additional reactions												
NH$_4$ assimilation[2]	13					−13						
Dissolution of [Al(OH)$_3$]$_s$	−6						6					
Final composition												
Calculated	5	7	5	39	4	1	6	44	16	7	25[4]	8
Measured September 1985	4	6	5	40	4	1	6	42	16	8	15	—
Lake Zota Weathering reactions												
4 µmole plagioclase (x = 0.25)	−5	3		2							13	5
0.5 µmole epidote (x = 0.5)	−2			2							1.5	1
2 µmole biotite (x = 0.75)	−5		2		3						6	2
1 µmole K-feldspar	−1		1								3	1
Additional reactions												
NH$_4$ assimilation[2]	7					−7						
NH$_4$ nitrification[5]	12					−6			6			
Dissolution of [Al(OH)$_3$]$_s$[3]	−9						9					−5
Final composition												
Calculated	13	7	6	31	6	1	9	44	22	7	23.5[4]	4
Measured September 1985	10	7	6	30	6	1	9	39	24	7	13	—

[1] Evapoconcentration factor = precipitation/runoff = 1.7 m/1.2 m = 1.42.
[2] NH$_4$ assimilation: NH$_4^+$ → (NH$_3$)org + H$^+$.
[3] Al(OH)$_{3s}$ + ν H$^+$ → Al(OH)$_{3-\nu}^{\nu+}$, ν depends on the pH of the lake water.
[4] Loss of H$_4$SiO$_4$ due to incorporation in diatoms, and adsorption on noncrystalline Al(OH)$_3$ not included.
[5] NH$_4$ nitrification: NH$_4^+$ + 2 O$_2$ → NO$_3^-$ + 2 H$^+$ + H$_2$O.

represent a mean for the soluble part of snow, rain, and dry deposition. In addition, a correction was made for the partial evaporation during runoff.

The contributions of the individual weathering reactions were assigned and combined in such a way as to yield the concentrations of Ca^{2+}, Mg^{2+}, Na$^+$, K$^+$, and H$^+$ measured in these lakes; the amounts of silicic acid and aluminum hydroxide produced and the hydrogen ions consumed were calculated stoichiometrically from the quantity of minerals assumed to have reacted. Cor-

rections must be made for biological processes (Schnoor and Stumm, 1985), such as ammonium assimilation and nitrification and the uptake of silicic acid by diatoms. Some of the H$_4$SiO$_4$ was apparently lost by adsorption on aluminum hydroxide and Fe(III)(hydr) oxides, but the extent of these reactions was difficult to assess.

Although an unequivocal quantitative mass balance could not be obtained, despite the uncertainties, a plausible reaction sequence was deduced that accounts rea-

sonably well for the residual chemical water composition. The amount of $CaCO_3$ that had to be dissolved to establish the residual water composition is about what can be accounted for by wind-blown calcite dust. The neutralization of the acidic precipitation by NH_3 was, subsequent to its deposition, largely annulled by the H^+ ions produced by nitrification and NH_4^+ assimilation.

According to Table 3, in the drainage area of Lake Cristallina, about 4 μmole of plagioclase, 2 μmole of epidote, 1 μmole of biotite, and 1 μmole of K-feldspar per liter of runoff water are weathered per year. This amounts to 19 meq of cations per m^2-year. The situation is similar for Lake Zota (16 meq of cations per m^2-year).

ACKNOWLEDGMENTS

REFERENCES

Berner, R. A. and Holdren, G. R., Jr. (1977) Mechanism of feldspar weathering: Some observation evidence: *Geology* **5**, 369–372.

Blum, A. and Lasaga, A. (1987) Monte Carlo simulations of surface reaction rate laws: in *Aquatic Surface Chemistry*, W. Stumm, ed., Wiley-Interscience, New York, 520 pp.

Cornell, R. M. and Giovanoli, R. (1987) The influence of silicate species on the morphology of goethite (α-FeOOH) grown from ferrihydrite ($5Fe_2O_3 \cdot 9H/_2O$): *Chem. Comm., J. Chem. Soc., London,* 413.

Fung, P. C. and Sanipelli, G. (1982) Surface studies of feldspar dissolution using surface replication combined with electron microscopic and spectroscopic techniques: *Geochim. Cosmochim. Acta* **46**, 503–512.

Furrer, G. and Stumm, W. (1986) The coordination chemistry of weathering: I. Dissolution kinetics of δ-Al_2O_3 and BeO: *Geochim. Cosmochim. Acta* **50**, 1847–1860.

Garrels, R. M. and Christ, C. L. (1965) *Solutions, Minerals and Equilibria:* Harper and Row, New York, 450 pp.

Günthert, A., Stern, W. B., and Schwander, H. (1976) Isochemische Granitgneissbildung im Maggia-Lappen: *Schweiz. Min. Petrogr. Mitt.* **56**, 105–143.

Heggie, M. I. and Zheng, Y. (1987) Planar defects and dissociation of dislocations in a K-feldspar: *Phil. Mag.* **A56**, 681–688.

Johnson, C. A. and Sigg, L. (1985) Acidity of rain and fog: Conceptual definitions and practical measurements of acidity: *Chimia* **39**, 59–61.

Keller, W. D. (1978) Kaolinization of feldspar as displayed in scanning electron micrographs: *Geology* **6**, 184–188.

May, H. M., Helmke, P. A., and Jackson, M. L. (1979) Gibbsite solubility and thermodynamic properties of hydroxy-aluminum ions in aqueous solution at 25°C. *Geochim. Cosmochim. Acta* **43**, 861–868.

Miller, W. R. and Drever, J. I. (1977) Chemical weathering and related controls on surface water chemistry in the Absaroka Mountains, Wyoming: *Geochim. Cosmochim. Acta* **41**, 1693–1702.

Mosello, R. and Tartari, G. A. (1987) Chemistry of atmospheric deposition at L. Toggia (2160 m a.s.l.), with emphasis on the sampling procedure: in *Proc. 4th Europ. Symp. Physico-Chemical Behaviour of Atmospheric Pollutants, Stresa, Italy, 1986,* G. Angeletti and G. Restelli, eds., Reidel, Dordrecht, 176–187.

Pavlova, V. and Sigg, L. (1988) Adsorption of trace metals on aluminium oxide: Simulation of processes in freshwater systems: *Water Research* (in press).

Robert, M., Cabidoche, Y.-M., and Berrier, J. (1986) Pédogenèse et minéralogie des sols de haute montagne cristalline (etages alpin et subalpin), science du sol: *Bull. Assoc. Franç. Etude Sol,* **4**, 313–336.

Schnoor, J. L. and Stumm, W. (1985) Acidification of aquatic and terrestrial systems: in *Chemical Processes in Lakes,* W. Stumm, ed., Wiley-Interscience, New York, 435 pp.

Schnoor, J. L. and Stumm, W. (1986) The role of chemical weathering in the neutralization of acidic deposition: *Schweiz. Z. Hydrologie* **48**, 171–195.

Sigg, L., Stumm, W., Zobrist, J., and Zürcher, F. (1987) The chemistry of fog: Factors regulating its composition: *Chimia* **41**, 159–165.

Stumm, W., Morgan, J. J., and Schnoor, J. L. (1983) Saurer Regen, eine Folge der Störung hydrochemischer Kreisläufe: *Naturwissenschaften* **70**, 216–233.

Stumm, W., Sigg, L., and Schnoor, J. L. (1987a) Aquatic chemistry of acid deposition: *Env. Sci. Technol.* **21**, 8–13.

Stumm, W., Wehrli, B., and Wieland, E. (1987b) Surface complexation and its impact on geochemical kinetics: *Croat. Acta* **60**, 429–456.

Tardy, Y. (1971) Characterization of the principal weathering types by the geochemistry of waters from some European and African crystalline rocks: *Chem. Geol.* **7**, 253–271.

Zobrist, J., Sigg, L., Schnoor, J. L., and Stumm, W. (1987) Buffering mechanisms in acidified alpine lakes: in *Reversibility of Acidification,* H. Barth, ed., Elsevier, Barking, United Kingdom, 95–103.